Journal of Crystal Growth 113 (1991) 669–680
North-Holland

Morphogenetical characterization of the Brazil twin appearing in $-X$ and Z' growth sectors of synthetic quartz crystals by X-ray topography

M. González-Mañas and M.A. Caballero

Dpto. de Estructura y Propiedades de los Materiales, Facultad de Ciencias, Universidad de Cádiz, Apto. 40, 11510 Puerto Real, Cádiz, Spain

Received 15 March 1991; manuscript received in final form 15 May 1991

This paper deals with the study of the Brazil twin which appears in $-X$ and Z' growth sectors of Y-bar synthetic quartz crystals by means of mainly X-ray traverse topographs. The origin of those Brazil twins is investigated and the twin domain structure is determined. As a result of twinning, growth defects, i.e., growth subsectors and growth subboundaries (GSBs), appear in the $-X$ growth sector. Those defects have been characterized. Correlating both twin domain and "new defects" a qualitative morphogenetical model is proposed.

1. Introduction

Lattice distortions and defects in natural and synthetic quartz crystals have been studied by several authors, as quartz is one of the most important hydrothermally grown crystals, due to its great technological importance. This paper intends to be a contribution to the characterization of growth defects in synthetic quartz crystals, since an exhaustive study of Brazil twins in synthetic quartz crystals has never been carried out.

Tsinober et al. [1] have reported the ocurrence of Brazil twins in synthetic quartz on r, major rhombohedron $\{10\bar{1}1\}$, and on $-X$, negative trigonal prism face $(\bar{2}110)$. In the latter case Brazil twins are suggested to be formed by an autoepitaxial intergrowth of the two enantiomorphic individuals. A rapidly growing X surface of the twin domain and a slowly growing $-X$ face of the substrate are exposed on the side of free growth; thus the necessary condition for the development of the twin is satisfied. Howewer, the Brazil twin domain extends also into the adjacent Z' growth sector. X-ray topographic contrast, i.e., boundary contrast, due to optical twins of this kind, was reported for the first time by the authors [2]. Two types of Brazil twin boundaries were established: (a) crystallographical boundaries, parallel to the $(0\bar{1}11)$ major rhombohedron plane, similar to those subsisting in natural crystals [3–5], exhibiting fringe contrast in the topographs, and (b) irregular and stepped non-crystallographical boundaries showing a much more complex diffraction contrast. $(0\bar{1}11)$ boundaries extend across $-X$ and Z' growth sectors, while irregular ones are exclusively restrained to the Z' sector. Thus, generally, twin domains are optically (cross polarizers) as well as topographically visualized in Z-plates as, what we have called, a "boot-like" morphology.

The aim of this paper is to establish where the twins exhibited by the $-X$ surfaces nucleate, by studying the distribution and the evolution of the twin domains along the main growth direction [001] in relation with other growth defects appearing in synthetic quartz crystals. Those Brazil twins also perturb the normal growth of crystals in which they occur, generating fundamentally growth subsectors in the $-X$ growth sector which have never been characterized.

The structure of the twin boundaries was investigated by the authors using X-ray section topography [6]. Diffraction patterns were analysed

according to the current theories to determine the possible "fault vector". Those patterns have recently been simulated by computing methods, showing a complete disagreement with the "theoretical" images expected in the case of the "fault vector" structure. This study will be the aim of a next publication.

2. Experimental details

2.1. Growth conditions

The studied *Y*-cut synthetic quartz crystals were grown under the following conditions: growth temperature $354 \pm 2°C$; average temperature gradient 12.8°C; pressure 1600 ± 50 bar and solvent 1M NaOH or 0.95M NaOH + 0.05M $LiNO_2$. The growth rate along the [001] direction was 0.45–0.55 mm/day · face.

2.2. Twin morphology

On $-X$ $(\bar{2}110)$ surfaces, *Y*-cut synthetic quartz crystals twinned with the Brazil twin law generally show several two-fold symmetry polyhedra of different sizes (1 μm to 1 cm) arranged parallel to the [124] direction. Some of those polyhedra reach the external *z* surfaces (maximum development), making it possible to observe the "boot-like" morphology on these surfaces. The morphological and microtopographical features of those polyhedra were already reported by the authors [7]. Fig. 1 shows the typical morphology of the so-called

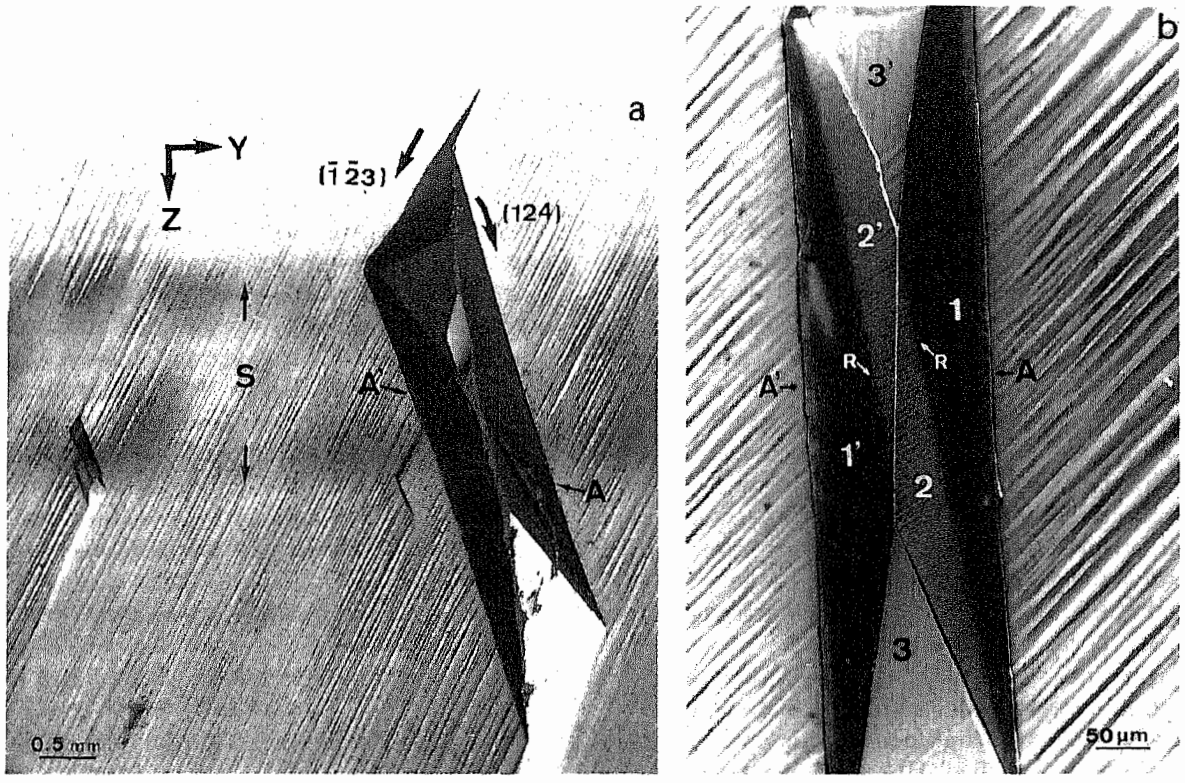

Fig. 1. Optical micrographs showing the characteristic morphology of the "basic polyhedra". (a) The orientation and distribution of polyhedra with respect to the seed crystal, S, can be observed. (b) A and A′ trapezoidal surfaces formed by 1, 2 and 1′, 2′ faces, respectively. R marks the two $(0\bar{1}11)$ Brazil twin boundary intersections extending over those surfaces. The rhombohedral 3 and 3′ faces complete this two-fold morphology.

"basic polyhedra". The Brazil twin domain extends across 2 and 2′ faces as has been determined in the present study.

The morphology of some polyhedra can be very complicated as a consequence of the overlapping of some "basic polyhedra".

2.3. Specimen preparation

To study the evolution of the twinned domain and the generation of the growth defects associated to twinning, several polyhedra of maximum development have been selected. Consequently, a series of Z-plates belonging to different polyhedra were sliced. Y-plates of other polyhedra were also prepared to study from another perspective those defects. All the crystals studied were right-handed. Equivalents polyhedra can also occur in left handed synthetic quartz crystals.

As usual, the plates were polished and etched in 45% HF solution for approximately 30 min. Twin domains appear on the surfaces as a result of different surface roughness. This fact, coupled with the optical activity, provides us with the possibility of comparing the topographic and optical results, facilitating in some occasions the determination of the twin domain morphology in all kinds of plates. The thickness of the different plates is approximately 0.25–1 mm.

Transmission X-ray topographs (Lang's method) were carried out using Mo $K\alpha_1$ radiation.

3. X-ray topography: results and discussion

Topographs of two series of Z-plates corresponding to polyhedra of different crystals are shown in figs. 2 and 3. All of them correspond to $\bar{2}110$ symmetrical reflection. As was to be expected, they bring out the similarity of the diffraction contrasts of the perturbed regions in both series. In order to clarify the exposition below, the distribution and evolution of defects are schematically represented in fig. 4.

3.1. Twin domain: evolution during growth

As already described above, a Brazil twin domain is clearly seen in the topographs of figs. 2 and 3 by boundary contrast. Let us analyse the extension and the evolution of the twin domain. In internal Z-plates (very close to the seed) the twinned individual extends across the $-X$ growth sector in a narrow band limited by two $(0\bar{1}11)$ boundaries. Traversing the $-X/Z'$ GSB, the twin morphology changes, corresponding always to triangular domains (sketched in fig. 4a), consistent with the point symmetry of the (0001) plane, whose boundaries are almost parallel to the prismatic planes $\{10\bar{1}0\}$. This can be observed in fig. 3a. Due to the high dislocation density, the corresponding twinned domain is not visible in fig. 2b.

As growth progresses, the twinned domain in the $-X$ growth sector shifts from left to right, consistent with the $(0\bar{1}11)$ boundary orientation, traversing different "zones" of the polyhedra. The triangular twins in the Z' growth sector spread and their boundaries progressively change their orientation until they get the typical "boot-like" morphology observed in intermediate and external Z-plates. Diffraction contrast due to the non-crystallographic boundary is getting more complex towards the external Z-plates. Steps showing fringe contrast almost parallel to the [100] direction can be observed in intermediate Z-plates (see figs. 2d, 2e and 3b). In the more external Z-plates it has frequently been observed that the left situated $(0\bar{1}11)$ twin boundary changes its orientation with respect to the [001] direction (see fig. 2f).

A $\bar{2}110$ reflection topograph corresponding to a Y-plate of another polyhedron of maximum development is shown in fig. 5. The twin domain morphology in Y-plates will depend, of course, on the region of the polyhedron being observed and also on the "structure" of the twinned individual, as will be seen below. Generally, the twin morphology shows an "L" shape, as in fig. 5, limited by the two $(0\bar{1}11)$ boundaries connected with the irregular ones, one of which coincides with the Z'/Z GSB.

It is important to note that Brazil twins never surpass the Z'/Z GSB, as all those topographs bring out.

3.2. Defects associated to Brazil twins

As can be observed in figs. 2, 3 and 4, new growth subsectors generated by the growth of the

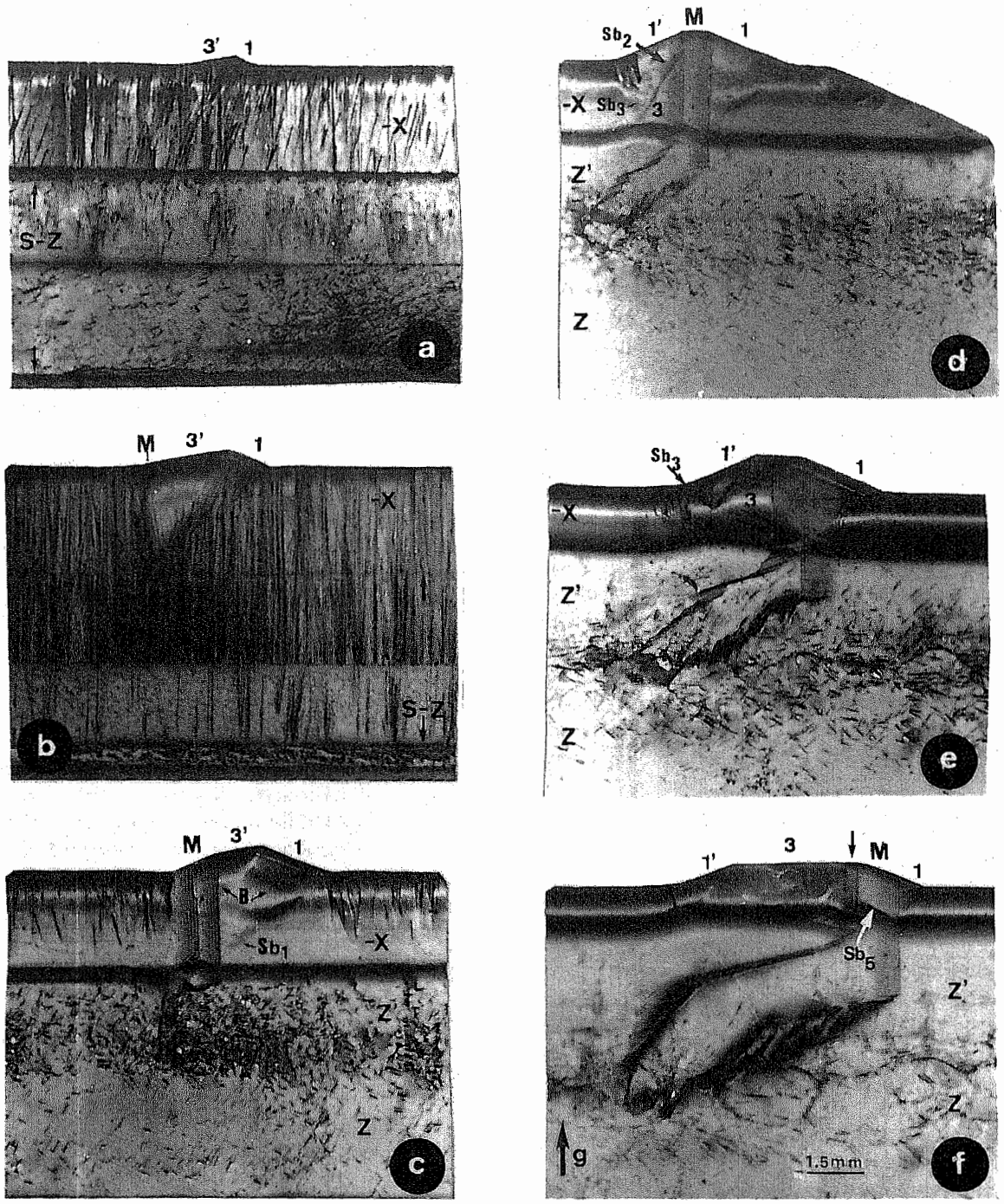

Fig. 2. Series of topographs of Z-plates corresponding to a polyhedron of maximum development of crystal QS-2. From (a) to (f) the polyhedron is examined from the more internal Z-plate, Z-7, close to the seed, to the more external, Z-2. They show the extension and the evolution of both twin domain and new defects. The twin domain, M, is revealed by boundary contrast. The two different twin boundaries are clearly seen. 1, 1', 3 and 3' mark the trapezohedral and the rhombohedral, respectively, growth subsectors (see text) and Sb_1 to Sb_5 the GSBs. The growth dislocations of the $-X$ growth sector are refracted traversing the Sb_1 GSB in the more internal Z-plates, see (a) and (b). The growth bands, B, almost parallel to $(\bar{6}51\bar{1})$ are seen in (c) and (d), those parallel to $(\bar{3}03\bar{1})$ can be seen in (c). In (f), the twin boundary marked with an arrow has changed its orientation with respect to the $(0\bar{1}11)$ plane. All of them correspond to $\bar{2}110$ symmetrical reflection.

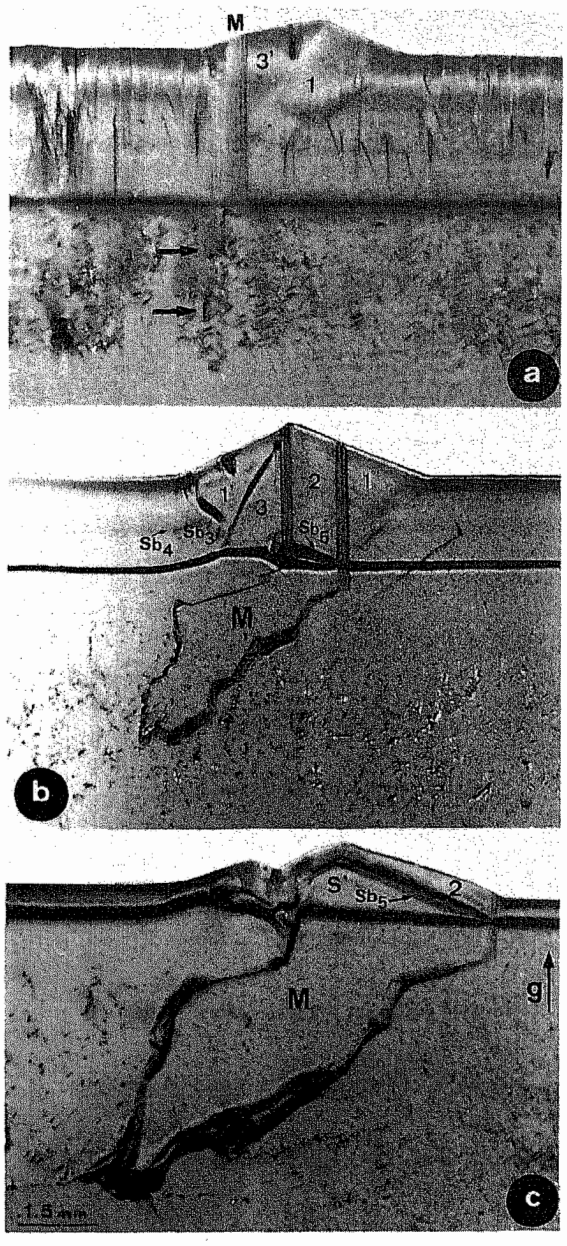

Fig. 3. Series of topographs of Z-plates of crystal QS-1 similar to the one of fig. 2. From (a) to (c), the plates are namely Z-3, Z-2 and Z-1. Twin domain and new defects show diffraction contrats very similar to those of fig. 2. Nevertheless, the triangular twin domains in the Z' growth sector are cleary visible, see arrows in (a); the Sb_4 GSB shows a faint contrast in (b) and the great development of the bipyramidal growth subsector s' in the twin domain can be seen in (c) . All of them correspond to $\bar{2}110$ symmetrical reflection.

Brazil twin into consideration appear in the $-X$ growth sector. The polyhedron faces 1, 3 and 1', 3' (see fig. 1) are a external manifestation of those growth subsectors.

In accord with Klapper's theory [8], growth dislocations closely follow the growth direction and are refracted in traversing a GSB. This phenomenon can be observed in figs. 2a, 2b and 3a. Moreover, the $-X$ growth bands also change their direction (see figs. 2c, 2d, 3a and 3b), confirming that the main growth direction has changed, thus generating the growth subsectors.

Goniometric measurements allow us to establish that the growth bands belonging to growth subsectors 1 and 3', which are visible in internal Z-plates, and the corresponding external surfaces are fundamentally parallel to the morphologically left negative trapezohedral plane $(\bar{6}51\bar{1})$ and to the rhombohedral plane $(\bar{3}03\bar{1})$, respectively. Diffraction contrast due to $(\bar{6}51\bar{1})$ and $(\bar{3}03\bar{1})$ growth bands is practically invisible for the following reflections: $0\bar{1}10$, $\bar{1}\bar{1}20$, $0\bar{1}11$, $01\bar{1}1$ and $0\bar{1}10$, $0\bar{1}11$, $01\bar{1}1$ and $1\bar{2}10$, respectively (although those results are not completely shown here, it can be observed for instance in figs. 6 and 8). The theoretical values of $\boldsymbol{g} \cdot \boldsymbol{u}$, shown in table 1, are in agreement with the previous results, $\boldsymbol{g}$ being the diffraction vector and $\boldsymbol{u}$ a vector parallel to the growth direction.

Taking into account the two-fold symmetry of the "basic polyhedra", we consider that the 1' subsector is approximately parallel to the trapezohedron plane $(\bar{6}151)$. Howewer, its structure is quite different from the one of subsector 1, at least in polyhedra of maximum development and much more complex: different growth regions and occasionally dislocation bundles can be observed. This complex structure can be seen in fig. 7.

At the begining of growth, subsector 3 is parallel to the rhombohedron plane $(\bar{3}301)$ due to the symmetry. As the polyhedron develops, subsector 3 may change from rhombohedral growth to bipyramidal, almost parallel to $(\bar{2}111)$. This variation in the growth direction may be responsable for the loss of the two-fold symmetry in polyhedra of maximum development, also perturbing the "normal" growth of the trapezohedral subsector 1', hence the different structure.

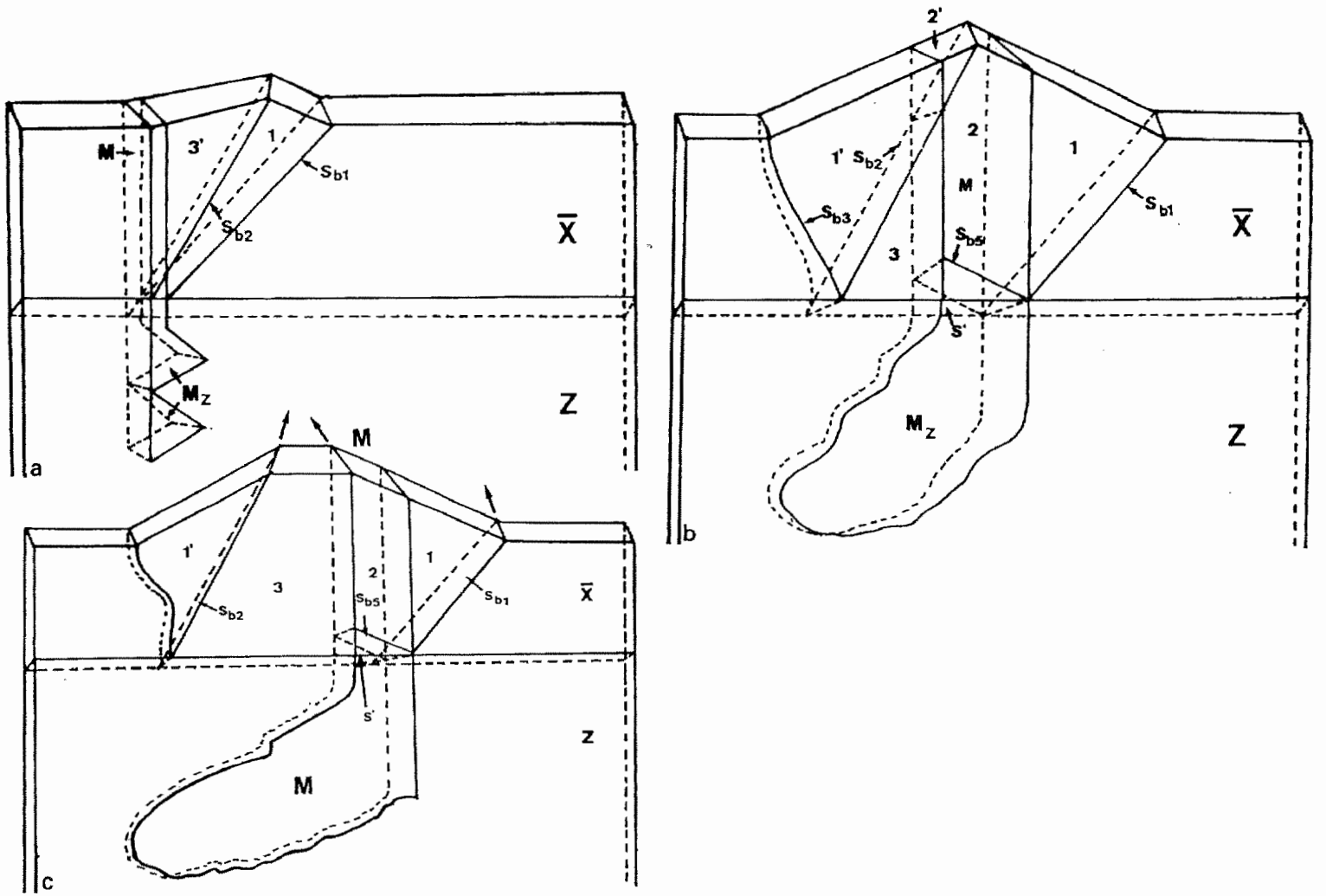

Fig. 4. The evolution of the twin domain and the defects associated with the Brazil twin are breafly sketched in three different stages of their development along the [001] growth direction. 2, 2′ and s′ constitute the twinned domain and 1, 1′, 3 and 3′ are the new growth subsectors. The different new GSBs, Sb_1 to Sb_5, are also drawn schematically.

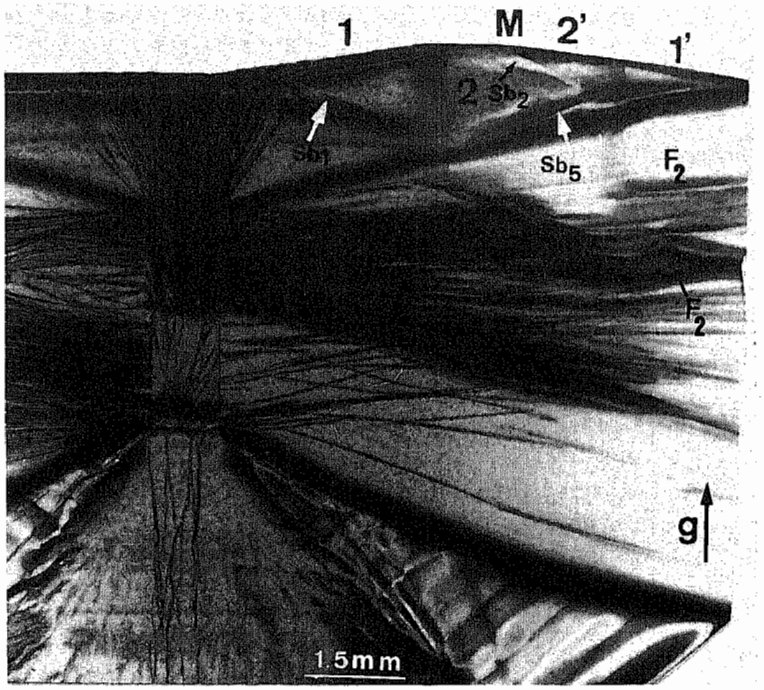

Fig. 5. Topograph of a *Y*-plate corresponding to another polyhedron of crystal QS-2 showing the structure of the twinned domain M (see text) and the new defects from another perpective. Fringe contrast, parallel to [100] direction, due to $(0\bar{1}11)$ boundaries and the complex contrast due to non-crystallographic boundary, F_2, are clearly seen. $\bar{2}110$ reflection.

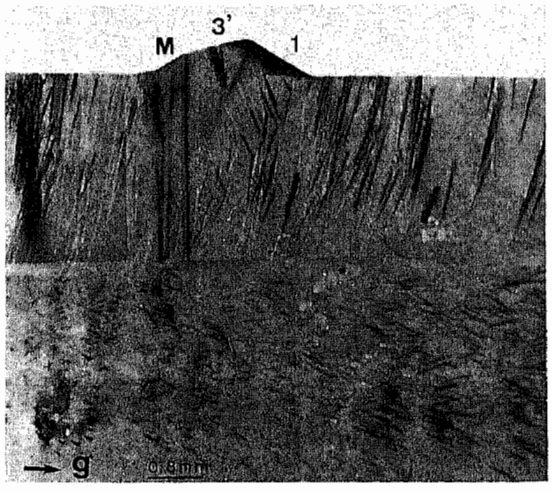

Fig. 6. Topograph of *Z*-3 plate of crystal QS-1 showing the invisibility of the 1 and 3′ growth bands. The inclined $-X$ dislocations exhibiting a black–white contrast are refracted traversing Sb_1 GSB. $01\bar{1}1$ reflection.

Fig. 7. Topograph of *Z*-4 plate of crystal QS-2 showing the different growth regions of trapezohedral subsector 1′ Sb_3 GSB exhibits a strong contrast and Sb_4 GSB is also visible. $0\bar{3}31$ reflection.

Table 1
Theoretical values of $\mathbf{g} \cdot \boldsymbol{u}$

Reflection	$[\bar{6}51\bar{1}]$*	$[\bar{3}03\bar{1}]$*
$0\bar{1}10$	−0.11	0.08
$\bar{1}\bar{1}20$	0.08	
$0\bar{1}11$	−0.15	0.05
$01\bar{1}1$	0.07	−0.12
$1\bar{2}10$		0

Growth subsectors are spatially limited by the twin boundaries themselves and by the characteristic GSBs that we call growth sector subboundaries, which can be observed for instance in figs. 2, 3 and 4.

The Sb_1 GSB separates subsector 1 from the $-X$ growth sector, while Sb_2 delimits subsectors 1 from 3′ and 1′ from 3, as well as subsectors 2 from 2′, which mainly constitute the twinned domain in the $-X$ growth sector, as will be shown below. Both GSBs can be considered planar faults inclined a few degrees with respect to the Z growth direction. They are not parallel to crystallographic planes of simple indices, which agrees with those results concerning the GSBs normally exhibited by synthetic quartz crystals (Parpia [9,10]).

The Sb_3 GSB, limiting subsector 1′ from the $-X$ growth sector, is a surface fault quite different from Sb_1 and Sb_2, as it changes its orientation during growth. Topographs of internal Z-plates bring out a "linear contrast" parallel to the [100] direction and differing from the one exhibited by the adjacent dislocations (see fig. 8). At the intermediate and the external Z-plates, the Sb_3 GSB corresponds to a curved surface fault which can be clearly seen in figs. 3b and 7. Thus the growth rate ratio between $-X$ and 1′ growth sectors varies during growth. Associated to this GSB, a dislocation bundle frequently appears in all the stages of its development. Both the orientation variation and the dislocation bundle allow us to distinguish between Sb_3 and Sb_1, Sb_2 GSBs with regard to their nature.

The change in growth direction from rhombohedral to bipyramidal during growth of polyhedra of maximum development also disturbs the normal growth of the $-X$ growth sector close to the 1′ subsector. Thus some regions of vicinal growth

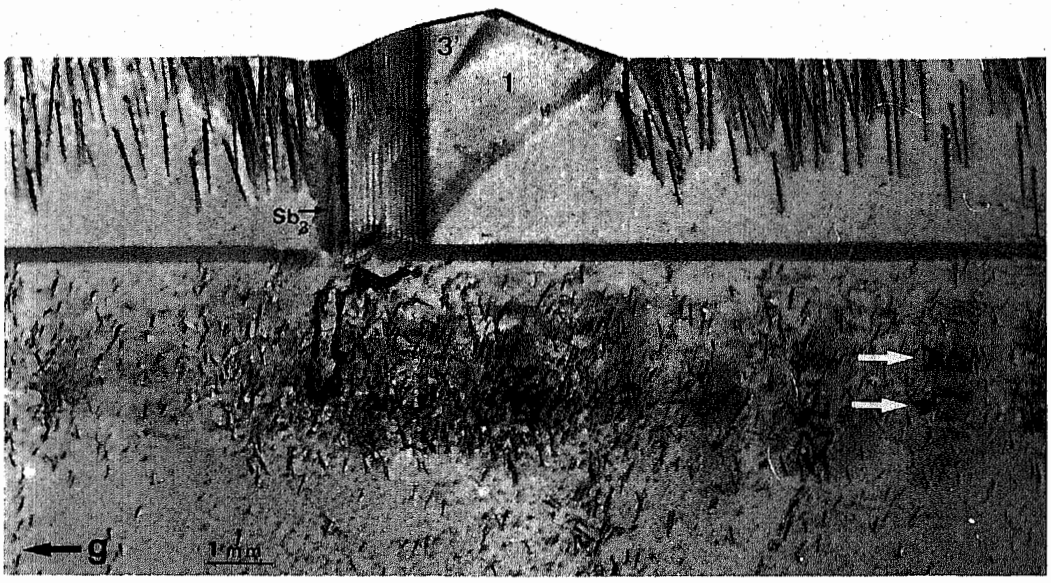

Fig. 8. Topograph of Z-5 plate of crystal QS-2 in which two triangular twinned microdomains, marked with two arrows, restrained to the Z' growth sector can be observed. They represent the first stages of the twinning generation at any moment during growth (compare with the other twinned domain in this plate). The growth bands in subsectors 1 and 3′ are invisible and Sb_3 GSB at its initial stage is clearly seen. $0\bar{1}10$ reflection.

can be generated and are delimited by other surface faults (see Sb_4 in figs. 3b and 7).

The twin domain structure is much more visible in topographs of Y-plates, due to the orientation of the twin boundaries. Those topographs bring out another perspective of defects under consideration. The twin domains in the $-X$ growth sector are mainly formed by two subsectors which externally correspond to the 2 and 2′ faces of those polyhedra (see fig. 1). They can be clearly observed in fig. 5 where a faint contrast corresponding to the Sb_2 GSB can be appreciated. The twofold symmetry of polyhedra and the twin boundary orientation, which allows us to assume that the twin law is a reflection across $(2\bar{1}\bar{1}0)$ plane, make us suggest that growth in subsectors 2 and 2′ is almost parallel to $(6\bar{1}5\bar{1})$ and $(6\bar{5}\bar{1}1)$, respectively. Some regions of growth parallel to $(2\bar{1}\bar{1}0)$ may also coexist.

In some polyhedra, the twinned domain in the $-X$ growth sector additionally exhibits a well-developed bipyramidal subsector s′, symmetric – due to the twin law – to the bipyramidal growth sector s (see fig. 9). This bipyramidal subsector s′ is located between $-X/Z'$ and another growth sector subboundary Sb_5. In Z-plates, the s′ subsector can be clearly observed in fig. 3c where the twinned domain spreads over the polyhedron and consequently the left situated twin boundary changes its orientation during growth.

Detailed observations of the diffracting contrast in the region of the twinned domain close to the $-X/Z'$ GSB bring out that there is always a planar fault similar both in orientation and in situation to Sb_5 described above (see, for instance, fig. 2f). This fact suggests that the s′ subsector is present in all the twinned domains with a different degree of development, which could be related to

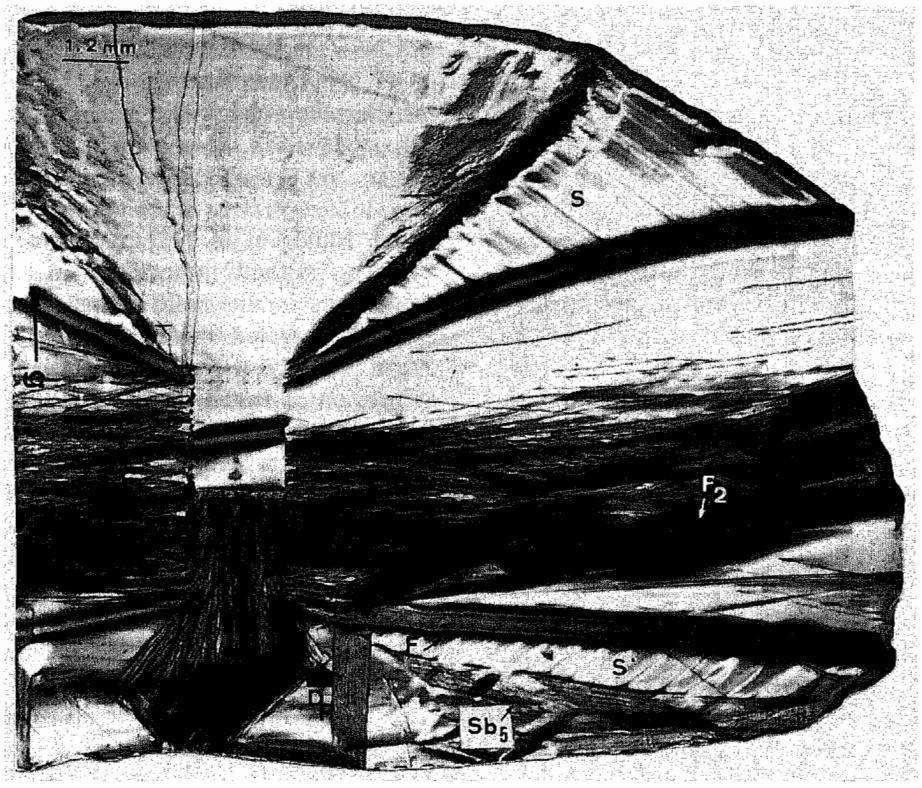

Fig. 9. Topograph of a Y-plate of crystal 431-III showing the great development of the bipyramidal subsector s′ in the twinned domain. The growth bands in s' are well developed and Sb_5 GSB, showing fringe contrast, is clearly seen. $1\bar{1}00$ reflection.

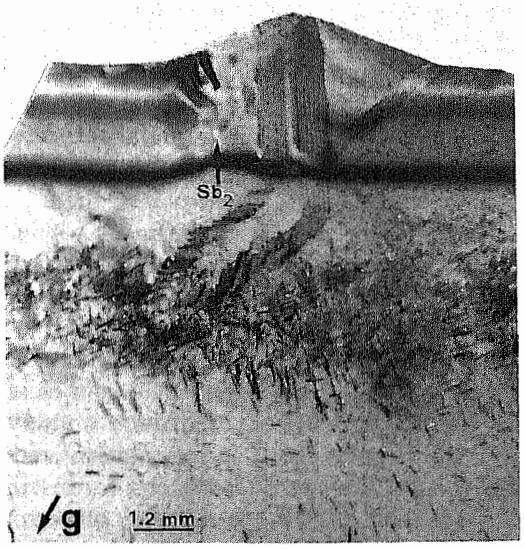

Fig. 10. Topograph of Z-4 plate of crystal QS-2 in which the Sb_2 direct image has vanished over its whole extension. $2\bar{2}00$ reflection.

the spreading of the twinned domain over the polyhedron.

In synthetic quartz crystals, the growth sector boundaries generally correspond to coherent lamelae [9–11]. Thus, diffraction contrast of a GSB of this type is originated by the misorientation and/or the different lattice spacing between the growth sectors and depends both on the inclination of the GSB with respect to the surfaces of the specimen and on the orientation of the diffraction vector with respect to the GSB intersections with those surfaces. Thus the direct image will be invisible when the diffraction vector is parallel to these intersections.

The GSBs under consideration generally show faint contrasts under all the diffraction conditions. Dynamic effects, i.e. fringes, predominate over kinematic ones, i.e. direct images, except for Sb_2 in the region in which it separates 1′ from 3 subsectors. The Sb_2 direct image vanishes in $1\bar{1}00$ type reflections (see for instance fig. 10), in agreement with the model of the coherent lamelae. Furthermore, those GSBs do not show evidence of dislocations.

Sb_2, separating 2 and 2′ subsectors in the twinned domain, shows an extremely faint contrast, see figs. 2d and 5, which may be explained by the fact that in those regions Sb_2 separates two crystallographically equivalent growth sectors.

3.3. Morphogenetical model

X-ray topography allow us to study the generation of the Brazil twin and how it is related to the "new defects" in order to suggest a qualitative morphogenetical model to explain the polyhedra observed on $-X$ grown surfaces.

The Brazil twins into consideration begin to generate in the high density dislocation region separating Z' from Z growth sectors (see, for instance, figs. 2, 3 and 5). Their first stages are triangular microtwins similar to those observed in fig 3a. This can be justified by the fact that triangular microtwins restrained to the Z' growth sector have been observed in some Z-plates (see arrows in fig. 8). Their geometry and situation are similar to those always exhibited by the more internal Z-plates of polyhedra (fig. 3a). This observation confirms that Brazil twins are generated in the Z' growth sector and it suggests that twins reaching the $-X$ growth sector start at the initial stages of growth. Moreover, Brazil twins confined to the $-X$ growth sector have never been observed.

Lu Taijing et al. [12] have shown that Brazil twins in synthetic amethyst generates either directly from smaller solid inclusions or from dislocations generated therefrom. According to this, Z'/Z GSBs constitute an ideal region for the generation of Brazil twins, since the high density dislocations supply the necessary strain field which provides sites where twin micronuclei can start to grow. According to Yoshimura and Khora [11], this high density of dislocations in Z'/Z GSB can be related to a high concentration of impurities, mainly interstitial Al, in those regions. Thus the existence of a highly distorted Z'/Z GSB is a necessary condition for the existence of Brazil twins.

It is by now clear that Brazil twins originate in the Z' growth sector at any moment during growth, thus the autoepitaxial intergrowth mechanism proposed by Tsinober et al. [1] cannot explain the formation of those twins, since this

growth direction is invariant with regard to twin symmetry. In this situation, twin nuclei are disabled to develop. This explains why there are some twin microdomains restrained to the Z' growth sector. Therefore, if twin micronuclei appear at the first stages of the growing crystal, located in the Z' growth sector and close to a $-X/Z'$ GSB, there will be some mechanism, problably related to the high distortion of this region, increasing the kinetics of propagation of those micronuclei in $-X$ growth direction.

The facts exposed above do not exclude the possilility that some twins would originate at the seed crystal.

Brazil twins reaching the $-X$ growth sector start their generation at the first stages of the crystal growth. This explains the fact that "basic polyhedra" observed on $-X$ growth faces are restricted exclusively to the central zones of those faces [7].

Different phenomena take place when the twinned nuclei reach the $-X$ growth sector. On the one hand, Brazil twins spread and develop by an autoepitaxial intergrowth mechamism [1]. The main growth direction in the twinned domain is now X [100]. In synthetic quartz crystals, the X grown surface is a multiheaded growth front [13], whereas [51$\bar{6}$1] trapezohedral growth bands are generally predominant. Our results bring out that the twinned domain located in the $-X$ growth sector is mainly constituted by two trapezohedral subsectors, ($6\bar{1}\bar{5}\,\bar{1}$) and ($6\bar{5}\,\bar{1}1$), corresponding to 2 and 2′ faces of polyhedra. Those results are thus consistent with the general mechamism of growth of the X growth sector.

On the other hand, the new growth subsectors start to grow in the $-X$ growth sector as a consequence of both twin symmetry and stability, since at the same time a rapidly and a slowly growing surface are exposed on the side of free growth. They correspond schematically to the trapezohedral faces ($\bar{6}51\bar{1}$) and ($\bar{6}151$) and to the rhombohedral faces ($\bar{3}03\bar{1}$) and ($\bar{3}301$) of the polyhedra. Under these conditions the twinned domain may develop within the Z' growth sector, getting its typical "boot-like" morphology as a result of both twin boundary orientation and growth direction in this sector.

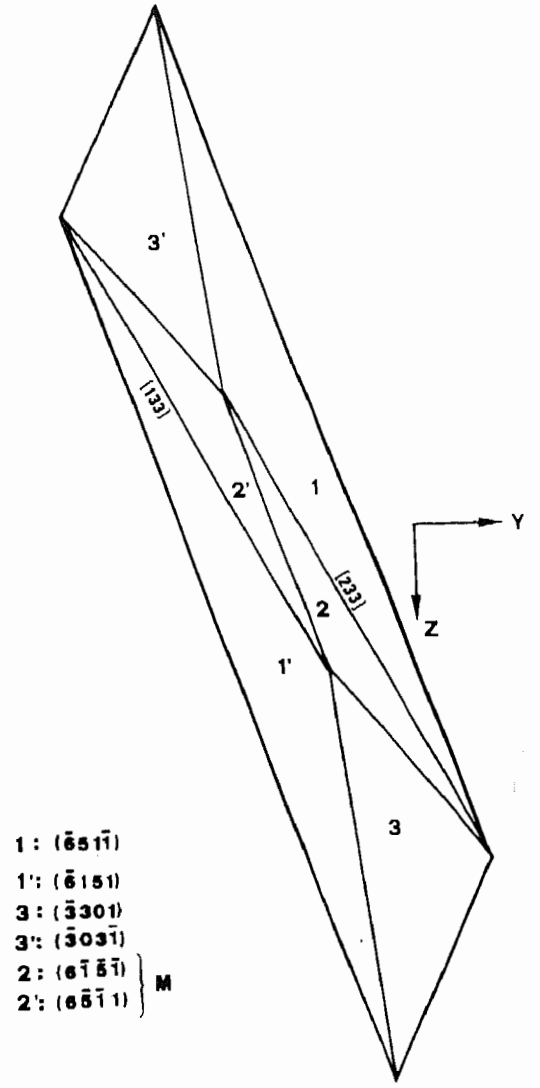

Fig. 11. Theoretically constructed model of the "basic polyhedron" projected onto the ($\bar{2}$110) plane. The external faces corresponding to subsectors 1, 1′, 2, 2′, 3 and 3′ are represented.

Fig. 11 shows the constructed "basic" polyhedron morphology projected on the ($\bar{2}$110) plane. This model has been drawn on the basis of both the theoretical lattice spacing planes corresponding to the experimentally determined surfaces and the orientation of the ($0\bar{1}11$) twin boundaries whose intersections with those surfaces are [233] and [133] directions. As can be observed, this

model is consistent with the morphology of the "basic" polyhedron.

4. Conclusions

The main results are briefly summarized in the following conclusions: (a) The Brazil twins appearing in $-X$ and Z' growth sectors generate in the Z'/Z growth sector boundary where there is a high density of dislocations. Their first "observable stages are triangular microtwins with boundaries approximately parallel to the prismatic planes $\{10\bar{1}0\}$ in the Z' growth sector. (b) The Brazil twins reaching the $-X$ growth sector start to generate in the first stages of the grown crystals. When the $-X$ growth sector has been attained, twins develop and the growth subsectors generate. (c) Both the twin domain and those new growth subsectors determine the final morphology of the polyhedra. The twin domain is fundamentally formed by two trapezohedral subsectors, $(6\bar{1}\bar{5}\bar{1})$ and $(6\bar{5}\bar{1}1)$, and the new growth subsectors appearing are the trapezehedral $(\bar{6}15\bar{1})$ and $(\bar{6}511)$, the rhombohedral $(\bar{3}03\bar{1})$ and the rhombohedral–bipyramidal $(\bar{3}301)$–$(\bar{2}111)$, the latter one depending on the degree of development of those polyhedra. (d) The twin domain morphology in the Z' growth sector changes during growth of polyhedra of maximum development. This originates from the "boot-like" morphology.

Acknowledgements

This paper has been carried out with the economic support of the DGICYT, PB87-0967. The crystals were provided by the SICN, Annecy, France.

References

[1] L.I. Tsinober, V.E. Khadzhi, L.A. Gordienko and M.I. Samoilovich, Growth of Crystals 6A (1968) 25.
[2] M.A. Caballero, M. González-Mañas and S. Dominguez, Bol. Soc. Esp. Mineral. 8 (1985) 9.
[3] P.P. Phakey, Phys. Status Solidi 31 (1969) 105.
[4] A.R. Lang and V.F. Miuscov, Growth of Crystals 7 (1969) 112.
[5] A.C. McLaren and D.R. Pitkethly, Phys. Chem. Minerals 8 (1982) 128.
[6] M. González-Mañas and M.A. Caballero, Bol. Soc. Esp. Mineral. 13 (1990) 19.
[7] M. González-Mañas and M.A. Caballero, Crystal Res. Technol. 23 (1988) K33.
[8] H. Klapper, in: Characterization of Crystal Growth Defects by X-Ray Topography, Eds. B.K. Tanner and D.K. Bowen (Plenum, New York, 1980) p. 133.
[9] D. Parpia, Phil. Mag. A 37 (1978) 375.
[10] D. Parpia, Phil. Mag. A 37 (1978) 401.
[11] J. Yoshimura and K. Khora, J. Crystal Growth 33 (1976) 311.
[12] Lu Taijing, I. Sunagawa and V.S. Balitsky, J. Crystal Growth 99 (1990) 1232.
[13] L.I. Tsinober, V.E. Khadzhi, L.A. Gordienko and L.T. Litvin, Growth of Crystals 14 (1984) 73.